

Following Coupled Electronic-Nuclear Motion through Conical Intersections in the Ultrafast Relaxation of β -Apo-8'-carotenal

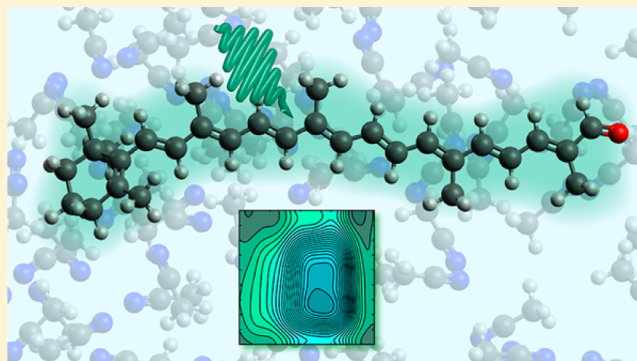
Thomas A. A. Oliver^{†,‡,§} and Graham R. Fleming^{*,†,‡,§}

[†]Department of Chemistry and [‡]Kavli Energy Nanosciences Institute, University of California, Berkeley, California 94720, United States

[§]Physical Biosciences Division, Lawrence Berkeley National Laboratory, Berkeley, California 94720, United States

Supporting Information

ABSTRACT: Ultrafast transient electronic absorption, one- and two-dimensional electronic-vibrational spectroscopies were used to study the nonradiative relaxation dynamics of β -apo-8'-carotenal (bapo), a model aldehyde containing carotenoid, in cyclohexane and acetonitrile solutions. 2D electronic-vibrational (2DEV) spectroscopy allows for a direct correlation between the intrinsically coupled electronic and vibrational degrees of freedom, which are thought to play an important role in driving relaxation of bapo from the bright S_2 and lower-lying dark S_1 state. Line shapes of features in the 2DEV spectra allow us to make more definitive assignments of excited state vibrations of bapo in acetonitrile. Anisotropy studies definitively demonstrate that the excited state dynamics of bapo do not involve a *trans*–*cis* isomerization, counter to prior hypotheses. For specific vibrational modes, the electronic and vibrational line shapes remain correlated beyond the decay of the S_2 excited state, indicating that the transfer of molecules to the S_1 state is impulsive and involves a conical intersection in the vertical Franck–Condon region.



1. INTRODUCTION

Carotenoids play a dual role in the photosynthetic machinery,¹ acting as efficient light harvesters^{2,3} and photoprotective radical quenchers;⁴ however, the nonradiative molecular mechanisms that underlie their functionality remain nebulous.^{5,6} The linear polyene chain of carotenoids is responsible for their strong visible absorption, and consensus has established the electronic transitions can be described in the C_{2h} point group.⁵ The precise number of ultrafast relaxation pathways from the optically bright S_2 ($1^1B_u^+$) state to the dark S_1 ($2^1A_g^-$) state is unclear: whether intermediate dark states of unknown electronic character participate (e.g., S^* , S_x , S^\dagger),^{5,7,8} or if ground state conformers give rise to a separate manifold of states^{9,10} remains widely debated.^{2,3,6} Carbonyl containing carotenoids, carotenals, form the most abundant subset of the polyenes in natural photosynthetic organisms. In environments such as polar solution or inside proteins, carotenals are able to access an intramolecular charge-transfer (ICT) state thought to be associated with the $C=O$ group that is conjugated with the polyene chain. A large number of studies have explored the nature of the charge-transfer state and whether it is connected to the S_1 manifold, or a completely independent electronic state.^{11–18}

The role of nuclear motions mediating the S_2 – S_1 coupling has been explored in several experimental and theoretical studies for β -carotene, and many groups have proposed that the crossing is driven by a conical intersection (CI) that links the S_2

and S_1 states.^{19–21} CIs provide an ultrafast funnel for nonradiative transfer between the two states and are formed when two electronic potential energy surfaces (PESs) intersect. CIs are constructed from two key coordinates: the tuning and coupling coordinates (the so-called g - and h -planes).^{22,23} Motion along the tuning coordinate first brings the states into degeneracy at the point of intersection. Continued movement in the same direction subsequently breaks this degeneracy. Typically, these modes are in-plane nuclear motions, as dictated by symmetry. The coupling mode(s) are out-of-plane nuclear motions that break the degeneracy of the states at every point on the intersection and provide the off-diagonal coupling mediating surface crossing. Experimental and theoretical studies for smaller polyenes (up to decapentaene) have shown that the $C=C$ and $C-C$ bond lengths are different for the minima on the S_0 , S_1 , and S_2 states. At the S_2 minimum, the $C=C$ and $C-C$ bond lengths become more even compared to S_0 ; i.e., the π -conjugation is more delocalized, whereas in the S_1 state, the bond orders are inverted compared to the ground state.²⁴ Pioneering *ab initio* studies by Garavelli, Olivucci, Robb, and co-workers for *trans*-hexatriene identified

Special Issue: Biman Bagchi Festschrift

Received: May 21, 2015

Revised: June 26, 2015

Published: July 1, 2015

the two key coordinates at the CI between the bright S_2 and dark S_1 states; slight displacement along a coordinate that lengthened the $C=C$ and shortened the C–C backbone bonds brought the S_2 and S_1 states into degeneracy, and out-of-plane backbone vibrations formed the coupling coordinate at the S_2/S_1 conical intersection.^{25,26} *Ab initio* calculations for polyenes with longer chain lengths become progressively more computationally expensive and unreliable due to an increased density of electronic states. The lack of high level *ab initio* calculations that can capture the photophysically relevant parts of the ground and excited PESs for carotenoids with chain lengths equal to β -carotene is a long-standing problem and would greatly assist interpreting time-resolved spectroscopies such as transient absorption^{7,11} or multidimensional electronic spectroscopy of carotenoids.^{8,13,27,28}

The nonradiative relaxation pathways of β -apo-8'-carotenol, a model carotenol (Figure 1a), have received a great deal of attention in the last 5 years and have been probed with transient absorption, transient infrared, transient-2D-infrared (*t*-2DIR), and femtosecond stimulated Raman spectroscopy (FSRS) techniques.^{16,29–35} In this study, we investigate the coupled electronic-vibrational relaxation from the S_2 state of β -apo-8'-carotenol (bapo) in cyclohexane and acetonitrile solutions using several different optical spectroscopies: transient absorption spectroscopy and broadband visible-pump, mid-infrared probe experiments. The latter we employ with far greater time resolution than previous studies.^{16,32–34} We also utilize two-dimensional electronic-vibrational spectroscopy (2DEV),³⁶ a technique that is uniquely placed to directly correlate the electronic and vibrational degrees of freedom, which are expected to be strongly coupled in carotenoids.^{20,37,38} From our combined studies, we are able to monitor the decay of bapo from the S_2 state and explore the role of CIs in the nonradiative decay in cyclohexane and acetonitrile solutions. Using polarization anisotropy measurements, we demonstrate that bapo does not undergo any immediate *trans*–*cis* isomerization along the polyene backbone on the excited potential energy surface, counter to previous studies of bapo,^{31,32} and other carotenoids.^{39,40} We observe correlated and anticorrelated electronic and vibrational transition frequencies in 2DEV spectra,^{41,42} for different vibrational modes on the excited states. From these different correlations, we are able to make far more rigorous assignments of the excited state vibrational frequencies in acetonitrile. For the $C=C$ antisymmetric stretching mode in acetonitrile, the time scale for loss of correlation between the electronic and vibrational degrees of freedom persists longer than the S_2 lifetimes determined in our transient absorption measurements and therefore provides direct evidence for the involvement of a conical intersection linking the S_2 and S_1 states of β -apo-8'-carotenol.

2. EXPERIMENTAL METHODS

a. Electronic-Vibrational Spectroscopy. Our one- and two-dimensional electronic-vibrational spectroscopy apparatus has been detailed previously.³⁶ Briefly, a Ti:sapphire oscillator (Micra, Coherent) seeded a commercial regenerative amplifier (Legend, Coherent, 1 W, 1 kHz, 40 fs) that was used to pump a home-built mid-IR optical parametric amplifier (OPA) and a visible non-collinear optical parametric amplifier (NOPA). The output of the NOPA (centered at 515 nm, 37 nm fwhm, Figure 1b) was compressed to 20 fs using an acousto-optic dispersive programmable filter (AODPF, Dazzler, Fastlite)⁴³ and

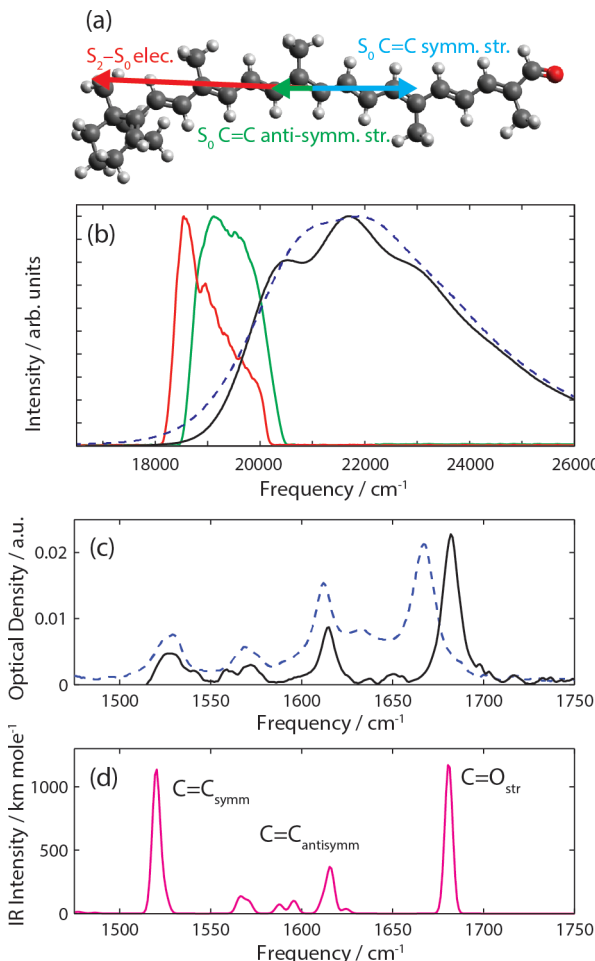


Figure 1. (a) Skeletal structure of *trans*- β -apo-8'-carotenol calculated at the B3LYP/6-311+G* level (see text for details). The overlaid arrows represent the calculated TD-DFT S_2-S_0 electronic (red) and fundamental ground state vibrational transition dipole moments for the $C=C$ symmetric (blue) and antisymmetric (green) stretch vibrations. (b) Linear absorption spectrum of bapo dissolved in cyclohexane (solid black line) and acetonitrile- d_3 (dashed blue line). The red and green lines display the pump laser spectra used to photoexcite molecules in visible and infrared probe measurements, respectively. (c) Solvent-subtracted linear mid-infrared absorption spectra of β -apo-8'-carotenol in acetonitrile- d_3 (dashed blue line) and cyclohexane solution (solid black line). (d) Calculated B3LYP/6-311+G* linear infrared absorption spectrum in cyclohexane (see text for details).

characterized by cross-wave polarized generation (Fastlite, Wizzler).⁴⁴ The AODPF pulse shaper was used to create a colinear pair of pump pulses, k_1 and k_2 , with time delay t_1 , and control the relative carrier-envelope phase, ϕ . The pair of pump pulses were focused into the sample with an $f = 25$ cm protected silver off-axis parabolic mirror (Optiforms). At the sample position, the pump pulses had a combined energy of 400 nJ and a spot size of 275 μm (16.8 GW/cm² per beam). The probe mid-IR laser output (centered between 5.8 and 6.5 μm) was split into roughly two equal parts using a ZnSe beamsplitter, creating probe (k_3) and reference mid-IR pulses. Both mid-IR reference and probe pulses were focused into the sample using an $f = 15$ cm protected gold off-axis parabolic mirror (Edmund Optics), but only the probe pulse was overlapped with the visible pump laser beam in the sample. The mid-IR pulses were compressed by addition of germanium

plates into the mid-IR beam path, to add negative group velocity dispersion.⁴⁵ The mid-IR pulse-duration was determined by cross-correlation with the visible pump beam in a thin germanium plate, returning pulse durations of ~60–100 fs. The mid-IR probe spot size was measured to be ~250 μm and ~100 nJ at the sample (~3.3 GW/cm²). The third-order nonlinear signal (\mathbf{k}_{sig}) is emitted collinear with the probe pulse from the sample. The mid-IR probe, signal, and reference pulses were collimated and imaged into a spectrograph (Horiba Triax) coupled to two 64-element HgCdTe detectors (Infrared Systems Associates). Normalization of signals with respect to the reference allowed for correction of shot-to-shot noise that is inherent to mid-IR laser pulse generation, and detection.

2DEV spectra were acquired for specific t_2 waiting times, and the t_2 delay was controlled by a motorized delay stage. Each 2DEV spectrum was collected by recording the normalized probe infrared spectral intensity (ω_3), modulated by \mathbf{k}_{sig} , as a function of the incremented t_1 time delays between \mathbf{k}_1 and \mathbf{k}_2 (0–100 fs in 1.19 fs steps), for four values of $\phi = 0, \pi/2, \pi, 3\pi/4$. Each combination of t_1 and ϕ was integrated for 50 laser shots and averaged ten times for each 2DEV surface. Every 2DEV surface was averaged for 5 scans. The frame of the pump pulses was fully rotated, and the 2DEV spectra obtained by applying a $4 \times 1 \times 1$ phase cycling routine to the $t_1-\omega_3$ surfaces. Fourier transform over the t_1 axis generated the resulting $\omega_1-\omega_3$ 2DEV correlation spectra.

One-dimensional visible pump, mid-IR probe data were acquired using the same apparatus and experimental conditions as detailed above, but the AOPDF was used to chop pump pulses.

The polarization of the visible pump pulses was controlled by a precision achromatic half-wave plate (Meadowlark). Anisotropy measurements were performed by sequential data acquisition with the relative polarization of pump and probe laser pulses set to 0 and 90°. The anisotropy, $R(t_2)$, was calculated as $(S_{\parallel} - S_{\perp})/(2S_{\perp} + S_{\parallel})$. All other data in this study were acquired in a parallel polarization configuration.

b. Transient Absorption. Degenerate broadband visible pump–probe experiments, henceforth referred to as transient absorption (TA), were performed using a slightly red-shifted NOPA laser spectrum (524 nm center, 32 nm fwhm, 25 fs; see Figure 1b for the laser spectrum). The NOPA was again compressed using the AOPDF pulse shaper, and split into pump and probe pulses with an achromatic beam splitter. For TA experiments, the pump and probe powers were set to 200 and 65 nJ, respectively, and focused to a 120 μm spot, with a combined power of 93 GW/cm² at the sample. The relative polarization of the pump and probe pulses was set to 0°. For these experiments, a mechanical chopper was used to block alternate pump pulses. The collinear probe and emitted signal were collimated and imaged into a spectrometer (SpectraPro 2300i, Acton Research Corporation) and frequency dispersed onto a CCD camera (Spec-10, Princeton Instruments). Nonresonant Raman scattering signals were removed by subtracting solvent only TA data.

c. Sample Preparation. β -Apo-8'-carotenal ($\geq 96.0\%$, Sigma-Aldrich) was kept at -19°C in the dark prior to experiments and used without further purification. β -apo-8'-carotenal was dissolved in acetonitrile (Sigma-Aldrich), acetonitrile- d_3 (D 99.96%, Cambridge Isotopes), and cyclohexane (Sigma-Aldrich) to create samples with optical densities of ~0.4 and ~0.3 at the central pump laser frequencies for mid-IR probe and visible probe experiments, respectively, in a 250

μm path length cell (2 mm thick CaF₂ windows, Harrick). See Figure 1b,c for the respective visible and mid-infrared absorption spectra. Samples were sealed and continuously circulated throughout data acquisition. All data were acquired at room temperature.

d. Density Functional Theory Calculations. The minimum energy geometries of the all *trans*- and *cis*-8' ground state conformations of β -apo-8'-carotenal were optimized using density functional theory (DFT) with the B3LYP exchange–correlation functional and a 6-311+G** basis set with an appropriate polarizable solvent continuum for cyclohexane and acetonitrile in the QChem4.1 computational suite.^{46,47} For the *all-trans* conformer, the vibrational normal modes and associated frequencies were also calculated. Time-dependent DFT (TD-DFT) with the same basis set and functional were used to calculate the S₂–S₀ transition dipole moment (TDM).

3. RESULTS AND DISCUSSION

a. Density Functional Theory Calculations. DFT calculations were used to investigate the ground potential energy surface for two different conformations of bapo: *cis*-8'-apo-8'-carotenal and *trans*- β -apo-8'-carotenal. The latter is displayed in Figure 1a, and the former conformer is formed by a 180° rotation of the C–C bond adjacent to the aldehyde group of the *all-trans*-conformer. At the B3LYP/6-311+G* level of theory in a polarized acetonitrile solvent continuum, the *cis*-8' conformer was calculated to be 1074 cm⁻¹ (~5 $\times kT$ at room temperature) higher in energy than the *all-trans* form. Previous studies have calculated the energies and transition states between several *cis*-isomers of bapo³⁹ along the middle of the polyene chain, and found that the barriers to interconversion are very high compared to kT (~8400 cm⁻¹). Studies have also demonstrated this for *cis*-isomers of β -carotene.^{10,48–50} Using these calculations as a guide, we are confident that the vast majority of bapo molecules will exist in the *all-trans* form at room temperature and therefore only consider the *all-trans* form throughout the rest of this study.

The ground state FTIR spectrum of β -apo-8'-carotenal in cyclohexane and acetonitrile- d_3 are displayed in Figure 1c, and the respective calculated DFT vibrational normal modes (multiplied by 0.97 to correct for any anharmonicity) are displayed in Figure 1d. The calculated frequencies and intensities are in good agreement with the experimental FTIR spectrum (Figure 1c), allowing for all the major peaks to be assigned. In cyclohexane, the peak at 1680 cm⁻¹ corresponds to the C=O stretch of the aldehyde group, and the band at 1530 cm⁻¹ to the C=C polyene backbone symmetric stretch. The modes at 1610, 1560, and 1570 cm⁻¹ correspond to mixed C=C antisymmetric stretches coupled with –CH₃ umbrella and C–H wag motions. In acetonitrile- d_3 (dashed line in Figure 1c), the vibrational line widths are broader, and the C=O stretch is shifted to a lower frequency, presumably due to stronger interactions with the more polar solvent. There is an additional band present in cyclohexane (at 1650 cm⁻¹) that has a significantly larger intensity in acetonitrile at 1630 cm⁻¹. Our DFT calculations predict a very low infrared oscillator strength for an isolated C=C stretch on the β -ionone ring at this frequency. The ground state assignments in our study are in general agreement with prior literature.^{31–33}

Overlaid on the skeletal structure of bapo in Figure 1a are the S₂–S₀ electronic TDM returned from TD-DFT calculations, and the ground state $\nu_{\text{C}=\text{C}}$ symmetric and antisymmetric vibrational TDMs. The directions of these the transition dipole

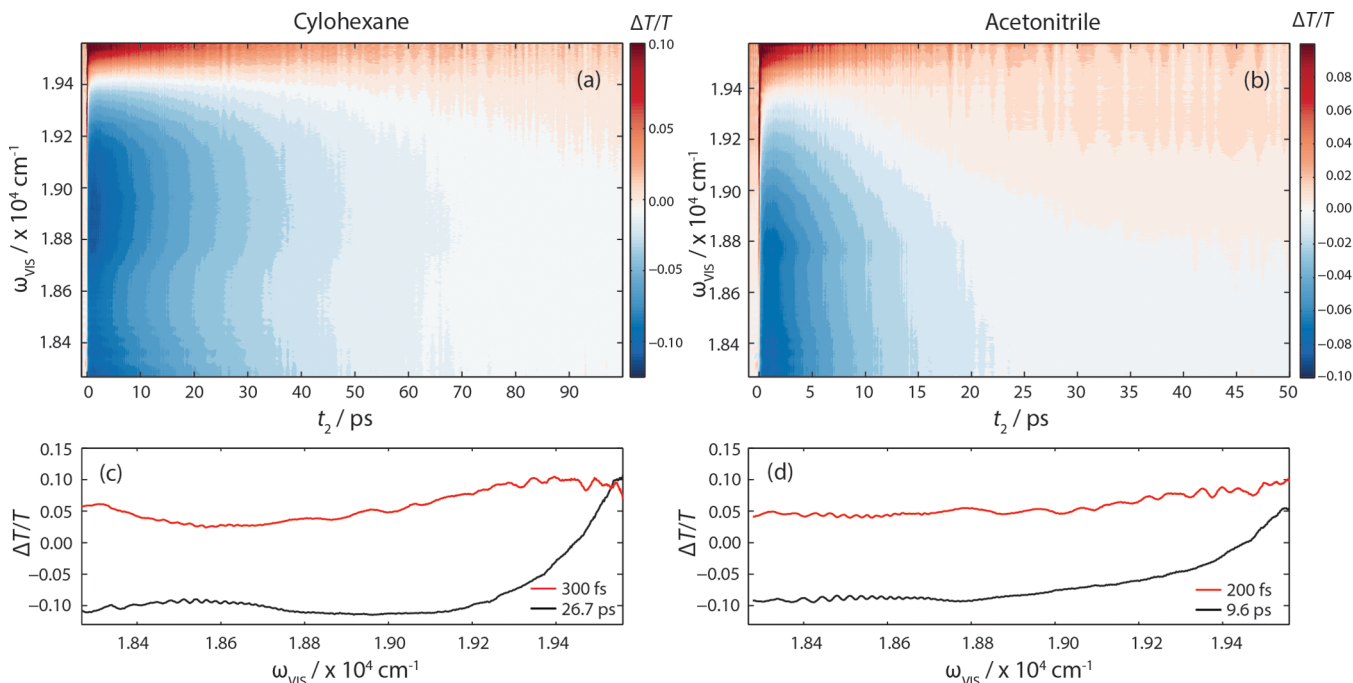


Figure 2. Transient absorption spectrum of β -apo-8'-carotenal in (a) cyclohexane and (b) acetonitrile solutions. Panels c and d display the decay associated spectra for the respective solutions.

moments are essential to understand correlations in 2DEV spectra presented in section 3c.

b. Transient Absorption. Parts a and b of Figure 2 display transient absorption spectra for bapo in cyclohexane and acetonitrile solutions. The spectra are dominated by two

Table 1. Decay Kinetics Obtained from Global Lifetime Analysis of Transient Absorption Measurements Using Pump Pulses Centered at 524 nm

solvent	lifetime components	
	τ_1/fs	τ_2/ps
assignment	S_2 lifetime	S_1 lifetime
cyclohexane	300	26.7
acetonitrile	200	9.6

features of opposite signs, which are well characterized for carotenoids and carotenals:⁵ positive signals at $\omega_{\text{VIS}} > 19200 \text{ cm}^{-1}$ correspond to ground state bleach recovery (GSB) and/or stimulated emission from the S_2 state. For $\omega_{\text{VIS}} < 19200 \text{ cm}^{-1}$, a broad negative transient dominates, attributed to $S_n \leftarrow S_1$ excited state absorptions (ESAs). Our degenerate electronic pump–probe experiments offer a superior instrument response (27 fs) than previous TA studies of β -apo-8'-carotenal;^{16,33} however, they do not stretch below $\omega_{\text{VIS}} = 18200 \text{ cm}^{-1}$, where in polar solutions the ESAs from the ICT state are expected to peak at $\sim 15400 \text{ cm}^{-1}$ ($\sim 650 \text{ nm}$).^{11,14,16}

The broadband degenerate TA data could not be analyzed in a self-consistent manner by fitting the decay of individual probe frequencies—the ground state absorption stretches almost the entire probe window, and overlaps with the very broad $S_n \leftarrow S_1$ ESAs. To decompose these components, a global analysis based on singular value decomposition was performed in the Glotaran software package.⁵¹ The kinetics for both data sets in the two solvents were fit to the same model, which assumes a sequential rather than a branched kinetic scheme. Our efforts to model

these data are slightly different compared to a recent study; we only required two decay components to model the data, rather than three,³³ and the error associated with these fits returned a RMS lower than 0.005 for both data sets. The spectrally resolved decay associated spectra (DAS) are shown in Figure 2c,d for bapo in cyclohexane and acetonitrile, respectively. The DAS component with an associated hundreds of femtoseconds time constant corresponds to a broad positive feature, assigned to stimulated emission from the S_2 state, or a direct branching to S_0 from S_2 , and therefore constituting a partial recovery of the ground state bleach. The second DAS component decays on a tens of picoseconds time scale and is predominantly a negative feature corresponding to $S_n \leftarrow S_1$ ESAs. We note that at higher probe frequencies a positive component is present, and we attribute this to ground state bleach recovery from the decay of the S_1 manifold. The specific lifetimes for the different decay components are given in Table 1 and are in agreement with previous literature values of the S_2 and S_1 lifetimes.^{29,32,33}

c. Electronic-Vibrational Spectroscopy. i. Cyclohexane. Figure 3 displays the one-dimensional broadband visible pump, mid-IR probe spectra for two probe regions of β -apo-8'-carotenal in cyclohexane (a, c). Contour maps comprising the entire 2D data sets are given in the Supporting Information. The spectra are almost exclusively dominated by negative bands, which correspond to excited state vibrations of bapo. The assignment of these different bands has been controversial,^{31,32} and the debate has centered on whether the central frequency of the vibrations associated with C=C and C=O bonds are shifted on the excited state compared to S_0 . Previous theoretical studies of smaller linear polyenes predict the frequencies of the backbone vibrations are significantly different on the excited states.⁵² The ground state frequencies are readily assignable with DFT calculations, however, as the excited PESs of carotenoids and carotenals still present a challenge to even cutting edge *ab initio* methods,^{53,54} and cannot be relied upon to quantitatively assign excited state

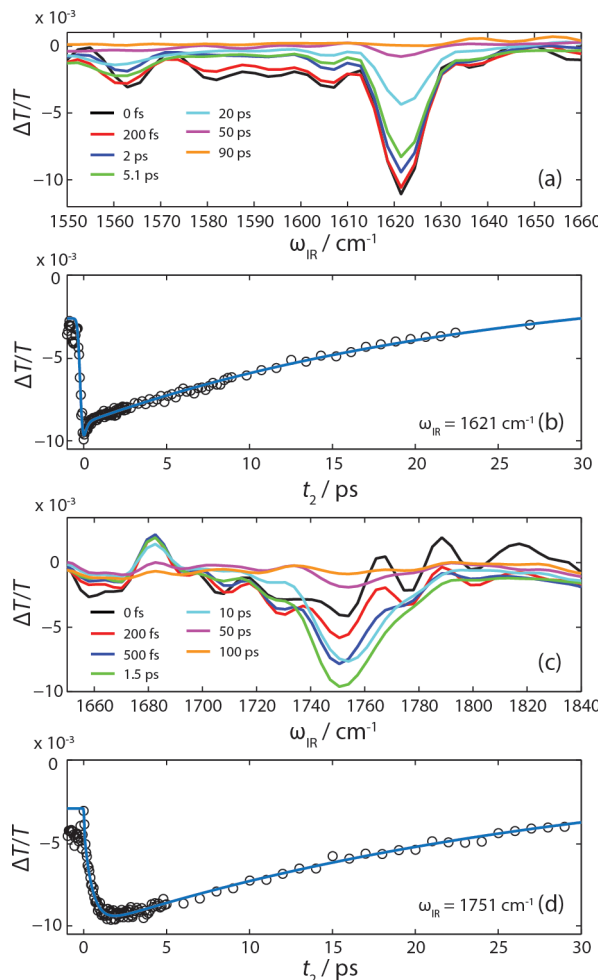


Figure 3. (a, c) Visible pump, mid-IR probe spectra for β -apo-8'-carotenal in cyclohexane at the displayed t_2 delays as a function of IR frequency. (b, d) Associated peak intensities and fits to data for selected probe frequencies.

vibrational frequencies. Pang et al. favored small shifts between S_0 and S_2/S_1 states of bapo; the vibrations are merely transposed from the ground to excited state, with slight shifts in frequency due to changes in force constants or anharmonicities on excited potential energy surfaces.³¹ Di Donato et al. favored a large blue shift for the C=C stretch ($\sim 100 \text{ cm}^{-1}$) and red shift for C=O vibration ($\sim 60 \text{ cm}^{-1}$) (cf. S_0), based on complete active space self-consistent field (CASSCF) calculations of a smaller chain apocarotenal.³² CASSCF does not treat dynamic electron correlation and

therefore is expected to poorly describe the electronic structure of the S_1 , and perhaps S_2 , states. More recent studies by the Righini group used FSRS³³ and 2D transient exchange IR³⁴ techniques. The FSRS measurement allows for a reliable identification of the excited state C=C stretch vibrational bands on the S_2 and S_1 states of bapo in cyclohexane. As we will show, visible pump mid-IR probe and 2DEV experiments bring into question the reliability of some of assignments extracted from 2D transient IR exchange measurements in polar solutions.³³

Our mid-IR pump–probe studies have a superior time resolution compared to previous studies,^{31–33} and that has the benefit of fewer experimental artifacts around $t_2 = 0 \text{ fs}$, such as cross-phase modulation. Figure 3a displays time traces for several t_2 time delays for the probe region where the S_0 C=C antisymmetric stretch vibrations are present in cyclohexane and are dominated by an excited state feature centered at $\omega_{\text{IR}} = 1621 \text{ cm}^{-1}$. Bleaching from the ground state C=C antisymmetric stretch vibration (1610 cm^{-1}) is expected in this region and can reconcile the slight dip on the red edge of this band. The 1621 cm^{-1} excited state vibration does not shift in frequency with increasing t_2 delays or show evidence of narrowing. The kinetics of the central frequency of the 1621 cm^{-1} feature are displayed in Figure 3b and show that the peak is present within the instrument response and therefore immediately projected onto the S_2 state. We favor assigning this peak to the C=C antisymmetric stretch, on the basis of its decay profile and proximity to its respective ground state bleach. The decay kinetics of this vibration, and all mid-IR features, are determined by the convolution of several factors. Negative t_2 dynamics, where infrared pulses precede the visible electronic excitation create vibrational coherences that are launched onto the excited (or ground) state, subsequently emitting an IR signal (see beating at $t_2 < 0 \text{ fs}$ in the 2D data plots shown in the Supporting Information),^{55,56} the instrument response function (70 fs for this IR probe frequency), and the relaxation dynamics of bapo in solution. To extract the relaxation dynamics, the data were fitted to a convolution of a Gaussian, to describe our IRF and the pretime zero IR signals, and a sum of two exponential decays. The returned time constants and amplitudes are given in Table 2, the fit is overlaid with the respective data, and returned 235 fs and 24.5 ps decay components. The biexponential decay is somewhat counter-intuitive; if the dominant relaxation channel is to transfer molecules from S_2 to S_1 , no decay would be observed. The initial ultrafast component may indicate a conical intersection in the vertical Franck–Condon region, directly funneling molecules back to S_0 , or to a lower lying dark state. An alternative explanation is the infrared transition dipole

Table 2. Decay Kinetics Obtained from Fitting Electronic-Vibrational Pump-Probe Spectra with the Pump Excitation Pulse Centered at 515 nm^a

solvent	band/cm ⁻¹	assignment	kinetic fit parameters			
			A ₁	τ_1/fs	A ₂	τ_2/ps
cyclohexane	1751	$\nu_{\text{C}=\text{C}}$ sym	0.38	500*	0.61	30.1
	1621	$\nu_{\text{C}=\text{C}}$ antisym	0.28	235	0.71	24.5
	1590	$\nu_{\text{C}=\text{O}}$ sym	0.71	201	0.28	22.5
acetonitrile- <i>d</i> ₃	1721	$\nu_{\text{C}=\text{O}}$ sym			1	8.5
	1675	$\nu_{\text{C}=\text{C}}$ sym			1	9.4
	1593	$\nu_{\text{C}=\text{C}}$ antisym	0.24	60	0.76	9.2

^aAll time constants were determined by fits to exponential decays, apart from the constant marked with an asterisk that was fit to a rise.

moments are weaker on the S_1 state than the S_2 state; the hundreds of femtoseconds time constant is similar to the lifetime of the S_2 state determined by TA experiments. The second decay constant is in good agreement with our TA DAS, assigned to the decay from S_1 . There is a weak but broad transient that decays with the similar time constants (Table 2), centered roughly at 1590 cm^{-1} , and from transient 2DIR exchange spectroscopy measurements in cyclohexane,³⁴ we can assign this to the excited state C=O symmetric stretch. The large change in fundamental frequency associated with the C=O bond on the excited state (the frequency is reduced by $\sim 70\text{ cm}^{-1}$), likely reflects a weaker C–O bond on the excited state. The bond order with respect to the carbon backbone is thought to reverse on the S_1 state (cf. S_0),²⁵ and the carbonyl group is conjugated with the polyene π system, and therefore the CO double bond may also acquire more single bond character. Notably, no excited state feature was observed near 1530 cm^{-1} , which corresponds to the S_0 frequency associated with the C=C symmetric stretch.^{31–33}

Figure 3c displays data for mid-IR probe measurements centered at 1750 cm^{-1} . At early time delays ($t_2 < 500\text{ fs}$) there is a broad negative feature (contaminated by bleaching at 1680 cm^{-1} by the S_0 carbonyl stretch) that spans 1660 – 1760 cm^{-1} and rapidly decays. At $t_2 > 500\text{ fs}$, a narrower transient at $\sim 1750\text{ cm}^{-1}$ rises. Both features in these data are very similar to transients observed in FSRS experiments of bapo in cyclohexane upon 400 nm excitation.³⁵ The transients in the FSRS study were assigned, by analogy to β -carotene,²⁰ to C=C symmetric stretches initially on the S_2 state, which are transferred to the S_1 manifold. Our fits to an exponential rise and decay of the 1750 cm^{-1} vibration (Figure 3d) yield a hundreds of femtosecond time constant, 500 fs , attributed to $S_2 \rightarrow S_1$ transfer, and a picosecond decay component, 30.1 ps , which we ascribe to relaxation back to S_0 . These decay constants are longer than those obtained from TA measurements (section 3b). This might be reconciled by overlapping ground and excited state features, the latter dominates the infrared probe spectra. The respective transient electronic absorption spectra, by comparison are far easier to decompose due to far less spectral congestion.

The width of the S_1 peak narrows between 500 fs and 10 ps (Figure 3c), presumably due to vibrational cooling on the S_1 state. Analysis of FSRS spectra that excited bapo at 400 nm ,³⁵ explained the change in line shape in terms of vibrational relaxation of multiple (up to 4) quanta of the C=C symmetric stretch in an anharmonic potential on the S_1 state. In our study, our pump excitation energy is far lower, near the S_2 absorption threshold and, therefore, the probability of directly exciting high vibrational levels of the C=C symmetric stretch vibration in S_2 , is lower. This difference in S_2 preparation can help reconcile the narrower line shapes in our spectra compared to the FSRS spectra.³⁵

Visible pump, mid-IR probe anisotropy measurements were used to investigate the time-dependent orientation of the excited C=C antisymmetric and C=C symmetric stretch vibrations, relative to the $S_2 \leftarrow S_0$ electric transition dipole moment of bapo, in cyclohexane solution. These data are shown in Figure 4. For both vibrations probed, $R(t_2)$ is positive and does not decay in the first 15 ps within the given signal-to-noise ratio. The different static values of $R(t_2)$ reflect the two backbone vibrations lie at slightly different angles pseudoparallel to the $S_2 \leftarrow S_0$ electronic transition dipole moment, as predicted by our TD-DFT calculated TDMs shown in Figure

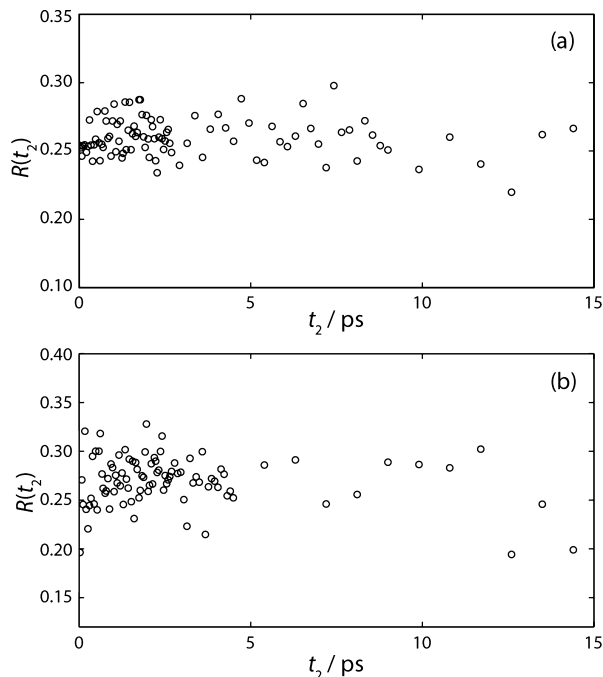


Figure 4. Anisotropy, $R(t_2)$, traces for (a) the C=C antisymmetric. (b) C=C symmetric excited state stretches of bapo in cyclohexane.

1a. The bright electronic TDM lies along the C_{2h} symmetry axis, in line with previous calculations for other polyenes.⁵⁷ The lack of time dependency in $R(t_2)$ is an important observation; conclusions from prior studies would predict that $R(t_2)$ should decay due to molecular reorganization, such as excited state *trans*–*cis* isomerization along the carbon backbone,^{30,39,40} but our data can definitively rule this out, demonstrating the polyene chain remains rigid on the excited state, not undergoing any permanent isomerization. One might expect rotational relaxation to induce a decay in $R(t_2)$ within the first 15 ps ; however, the electronic and vibrational transition dipoles investigated lie close to the C_{2h} axis of bapo, Figure 1a. bapo is an extreme prolate symmetric top, and rotational relaxation around the C_{2h} axis is therefore expected to be slow compared to the excited state lifetime.⁵⁸

We now turn to the two-dimensional electronic-vibrational spectroscopy measurements for the same probe regions investigated in the pump–probe studies. The main advantage of this technique over its one-dimensional counterpart is that it allows for a direct correlation between the initial electronic (visible) excitation energies and the subsequent vibrational (mid-IR) emission, forming a $\omega_{\text{vis}}-\omega_{\text{IR}}$ correlation spectra.³⁶ 2DEV spectroscopy is uniquely placed to explore the coupled electronic-vibrational dynamics that underlie the decay from the S_2 state of bapo and investigate the influence of conical intersections in the ensuing nonradiative processes.

Figure 5 displays real total 2DEV spectra for the 1621 cm^{-1} C=C antisymmetric stretch excited state vibration of β -apo-8'-carotenal in cyclohexane for four different waiting times. The main feature in these data is elliptical with no correlation between the electronic and vibrational frequency distributions and displays little evolution for larger values of t_2 .

Figure 6 shows the same data as Figure 5, but probing the S_1 excited state C=C symmetric stretch at 1750 cm^{-1} . As per our pump–probe spectra, the feature at $\sim 1750\text{ cm}^{-1}$ rises in the first few hundred femtoseconds; however, 2DEV spectra reveal

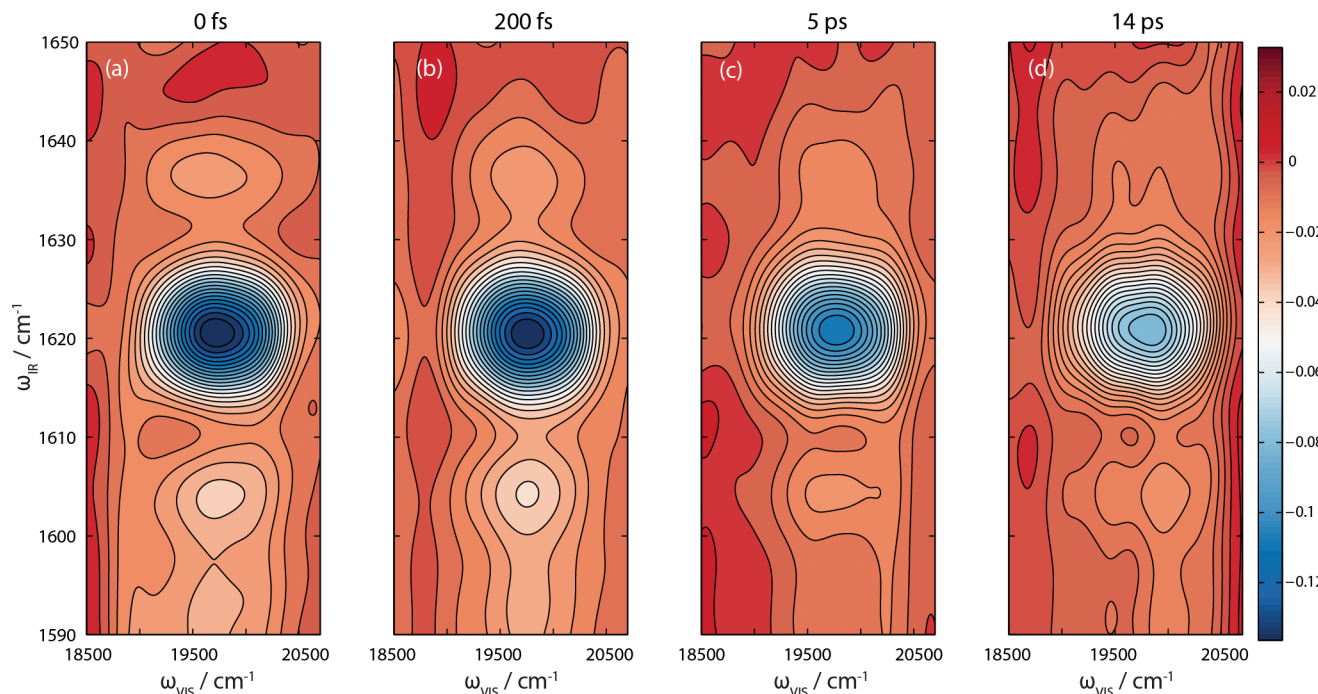


Figure 5. Real total 2D electronic-vibrational spectra for the C=C antisymmetric stretch of bapo in cyclohexane for the displayed t_2 time delays.

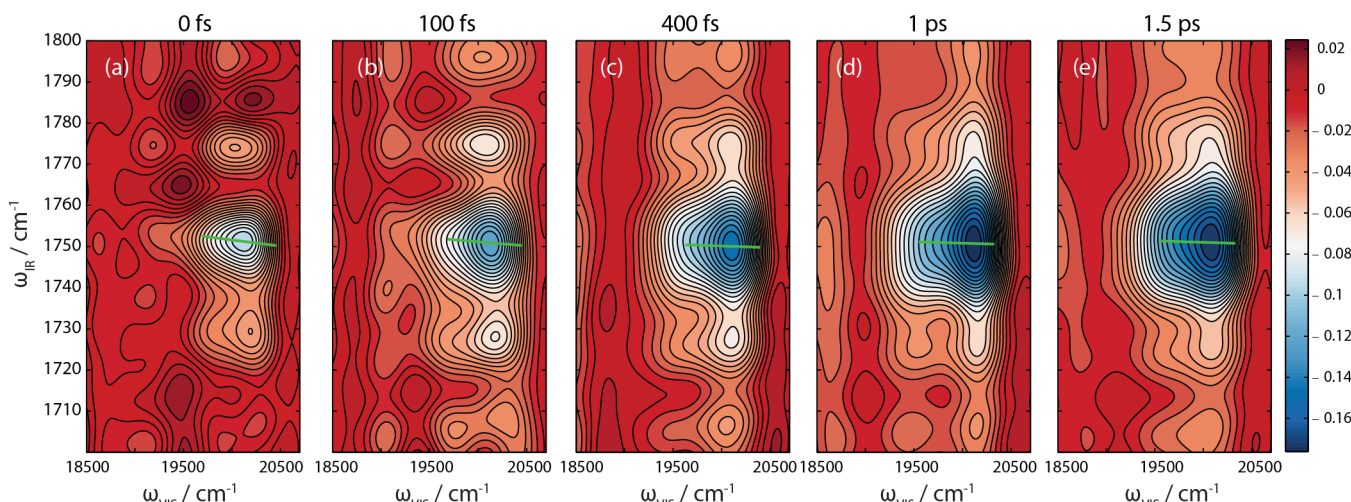


Figure 6. Real total 2D electronic-vibrational spectra for the C=C symmetric stretch of bapo in cyclohexane and displayed t_2 time delays. Green horizontal line shows the fitted center line slope (k_e).

a negative correlation between electronic and vibrational degrees of freedom. In other words, higher electronic excitation is correlated with lower vibrational frequencies.⁴¹ The line shape evolution can be characterized by the center line slope, which is directly proportional to the pump and probe frequency–frequency correlation function.^{59–61} In 2DEV spectroscopy, the pump and probe pulses are nondegenerate and thus the slope is different with respect to the ω_{VIS} and ω_{IR} axes. We define the two center line slopes (CLSs) for the excited state vibration as $k_e = d\omega_{IR}/d\omega_{VIS}$ and $k'_e, d\omega_{VIS}/d\omega_{IR}$.⁴² For this data set, we fitted the horizontal center line slope, k_e , for each 2DEV spectra at different t_2 delays. The respective fits are superimposed on 2DEV spectra in Figure 6. The vertical CLS, k'_e , was found to very close to zero.

Figure 7 plots the extracted values of k_e as a function of increasing waiting time, for the S_1 C=C symmetric stretch.

The decay of k_e as a function of t_2 , was fit to an exponential decay plus an offset, and returned $\tau = 300$ fs, similar to the S_2 lifetime determined by our TA studies (Table 1). As the S_1 vibration rises, it remains initially correlated with the initial S_2 excitation energy, meaning that the excited state $S_2 \rightarrow S_1$ surface crossing cannot involve any significant vibrational redistribution on the S_2 state and surface crossing must be ballistic; as expected for a mechanism involving a conical intersection. The S_2 – S_1 energy gap is estimated to be on the order of 7000 cm⁻¹,⁶² and therefore, equilibration on the S_1 state involves a large reorganization energy that, as evidenced via the decay of the CLS, destroys the electronic-vibrational correlation. We note that the center line slope for this feature, within our signal-to-noise ratio, does not reach zero and has a long-time offset that may arise from a small static inhomogeneous broadening component.

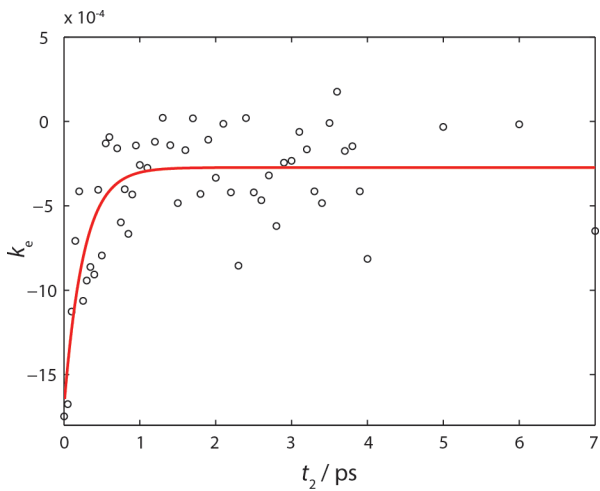


Figure 7. Excited state center line slope (k_e) for the S_1 C=C antisymmetric in cyclohexane as a function of t_2 .

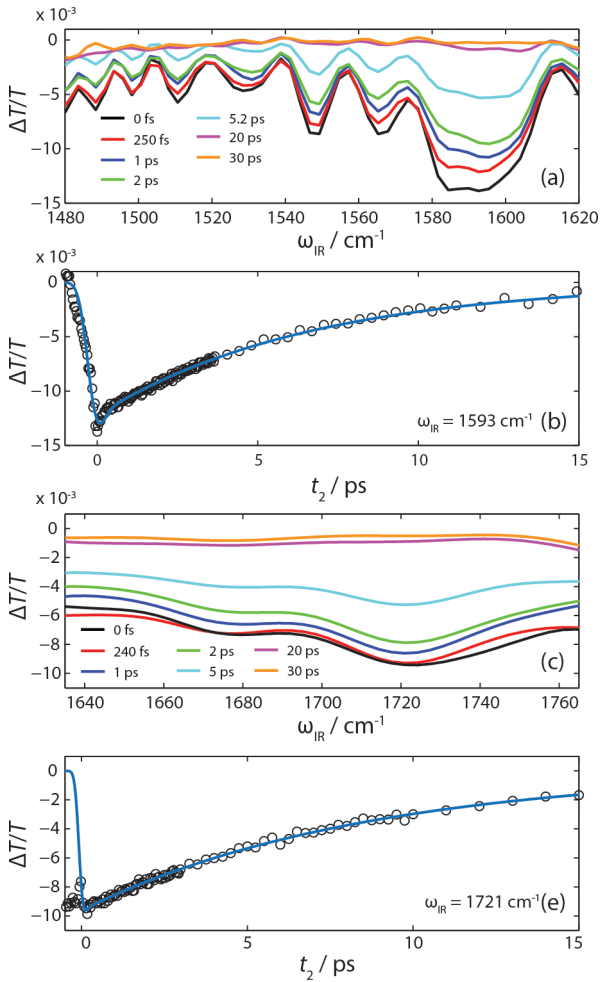


Figure 8. (a, c) Visible pump, mid-IR probe spectra for β -apo-8'-carotenol in acetonitrile- d_3 at the displayed t_2 delays probing the displayed IR frequencies. (b, d) Associated peak intensities and fits to data for the 1593 and 1721 cm^{-1} , respectively.

Our recent study of center line slopes in 2DEV spectra for a model two electronic level system demonstrated that the main factor determining the loss of correlation between electronic and vibrational degrees of freedom was vibrational dephasing

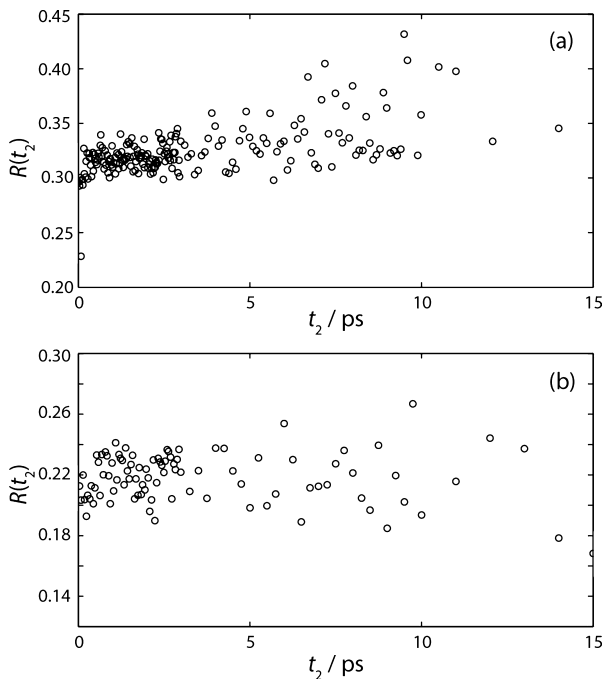


Figure 9. Anisotropy, $R(t_2)$, traces for (a) the C=C antisymmetric (b) C=O symmetric excited state stretches of bapo in acetonitrile- d_3 .

(typically on the order of several picoseconds).⁴² This allowed us to extract the relative coupling strengths of specific vibrational modes to the bath. Unfortunately, that is not possible here, as the S_2 lifetime of bapo is far shorter than the known vibrational dephasing time scale associated with the high frequency carbon backbone (or C=O) vibrations and, therefore, the model is unable to extract these coupling constants from k_e or k'_e . Physical insights can, however, be gained from the correlated (positive slope) or anticorrelated (negative slope) nature of the CLS, and the associated decay time scale.

2DEV spectra probe the cross-peak between electronic and vibrational transition frequencies. Diagonal peaks in degenerate 2DES and 2DIR spectra are initially positively correlated in the absence of significant homogeneous broadening. Cross-peaks between diagonal features, however, can be positively or negatively correlated, and theory has shown this to arise from correlated or anticorrelated bath fluctuations, respectively.^{63,64}

The electronic and vibrational transition frequencies are initially anticorrelated for the C=C symmetric of bapo in cyclohexane (Figure 6), as extracted from the CLS (Figure 7). The anticorrelation can be rationalized on similar grounds to previous 2DES and 2DIR studies. The physics that underlies the anticorrelated baths can be understood by considering the direction of the electronic S_2-S_0 TDM and the respective vibrational TDMs (Figure 1a). The S_2-S_0 electronic, and $v_{C=C}$ symmetric vibrational stretch TDMs are antiparallel with respect to one another and will polarize their respective baths in opposing directions. The cross-peak between these two transitions therefore yields an anticorrelated peak line shape.

ii. Acetonitrile- d_3 . Our measurements for the same probe vibrations in the polar acetonitrile- d_3 solvent are remarkably different to those observed for cyclohexane. Figure 8a displays data for $1480 \leq \omega_{\text{IR}} \leq 1620\text{ cm}^{-1}$. The major peak in the pump-probe spectrum centered at 1593 cm^{-1} , has been assigned to the C=O excited state stretching mode in

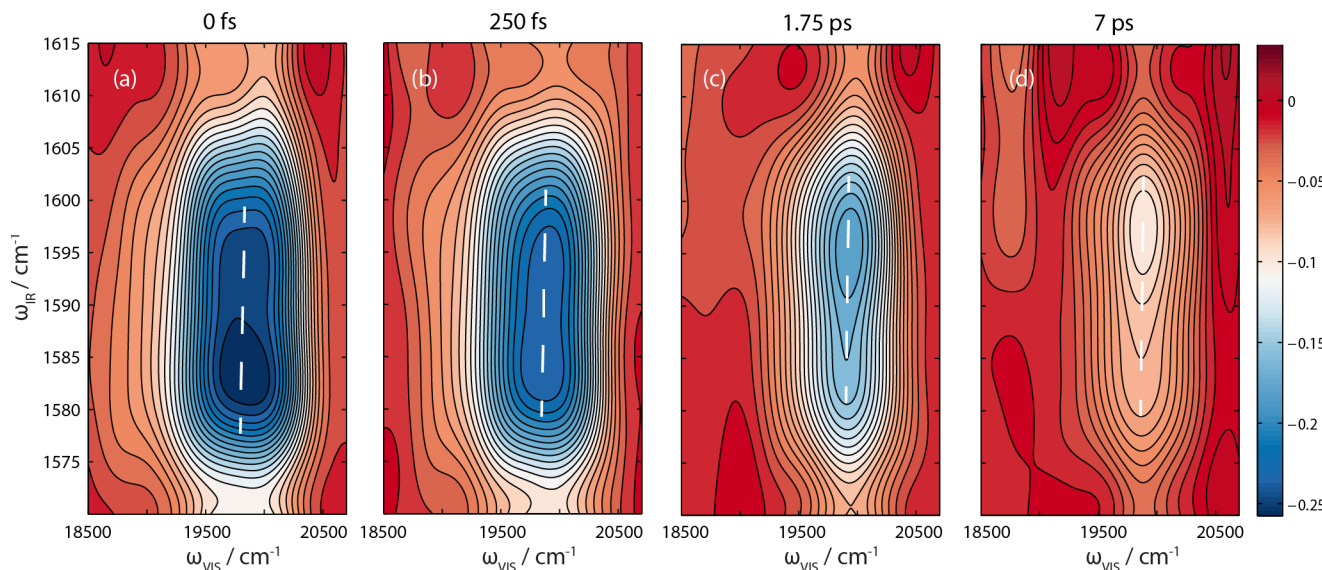


Figure 10. Real total 2DEV spectra for the C=C antisymmetric stretch of bapo in acetonitrile-*d*₃ for the displayed *t*₂ waiting times. Dashed lines indicate the center line slope.

chloroform,³⁴ however, due to spectral congestion, the assignments are not as definitive as in cyclohexane. The kinetics of the 1593 cm⁻¹ vibration are displayed in Figure 8b and, like in cyclohexane, the feature is immediately present on the excited state within the instrument response. The constants and amplitudes extracted from the decay of the feature are tabulated in Table 2. Our data display no sign of an ultrafast frequency shift for this mode in contrast to previous pump–probe data.³³ We observe, however, a slight blue shift of the central frequency associated with this vibration on a picosecond time scale. By analogy with our cyclohexane assignment, and from line shapes in 2DEV data (see below), we assign this feature to the excited state C=C antisymmetric stretch vibration.

Data for 1635 ≤ ω_{IR} ≤ 1765 cm⁻¹ are given in Figure 8c, and the region is dominated by two broad peaks, consistent with prior mid-IR probe studies.^{5,31,33} The kinetics for the peak of the feature at 1721 cm⁻¹ are displayed in Figure 8d. The pretime zero signals for this feature are intense and omitted from fits. The peak of the feature was fitted to a convolution of a Gaussian IRF with a single exponential decay, but unlike the respective signals for cyclohexane, no rise component was observed. The feature centered at 1721 cm⁻¹ narrows for larger *t*₂ values (compare traces at *t*₂ = 0 fs with 5 ps). The widths of the features are far broader than in cyclohexane, and acetonitrile has a large dielectric constant (37.5) and is able to significantly interact with the polar aldehyde group and accommodate an intramolecular charge-transfer state.^{5,11} A recent theoretical study of line shapes in electronic-vibrational spectroscopy predicted that the infrared line shape will be significantly broadened on electronic states with significant CT character, as the vibration acquires more dispersive character of the electronic state.⁶⁵ Guided by this theoretical prediction, and from the line shapes in the 2DEV spectra (see later), we assign the 1675 cm⁻¹ vibration to the C=C symmetric stretch vibration, and the smaller feature centered at 1721 cm⁻¹ to the carbonyl stretching mode.

We note that both the C=O and C=C symmetric stretch vibrations are broad. The structure in Figure 1a suggests the C=C and C=O bonds are likely conjugated, and we postulate

that the vibrational line shapes associated with these two modes are wide because the ICT state involves moving charge from the polyene backbone to the carbonyl group. The C=C antisymmetric stretch vibration is far narrower (Figure 7), because the antisymmetric stretching vibration breaks the aromatic character of the π network. The time dependence is revealing also: the transients in Figure 8 are immediately very broad, indicating that CT character is immediate with respect to these vibrational normal modes on the S₁ and (perhaps even S₂) electronic state(s), lending support to the hypothesis that the S₁ and ICT states are not two independent electronic manifolds with a barrier to crossing, but a single potential energy surface with mixed valence/charge-transfer character in polar solvents.^{5,12}

Figure 9 displays pump–probe anisotropy data for bapo in acetonitrile-*d*₃, which are reminiscent of the corresponding data in cyclohexane solution (Figure 4). The R(*t*₂) traces do not decay with increasing *t*₂ delays but have slightly smaller static values. This reflects the influence of the solvent on the S₂ ← S₀ electronic transition dipole moment and/or backbone vibrational TDMs compared to cyclohexane (Figure 4). Further, the lack of any decay in R(*t*₁) demonstrates, like in cyclohexane, bapo does not *trans*–*cis* isomerize on the excited state. This is counter to the claims of prior studies that have proposed 20–30° distortion/twist of the polyene of bapo and other carotenoids in polar solutions.^{32,33,39,40}

Real total 2DEV spectra for the peak at 1593 cm⁻¹, assigned to the excited state C=C antisymmetric stretch, are shown in Figure 10 for the displayed *t*₂ waiting times. The 2D line shape shows a dramatic evolution with increasing waiting times; the central IR frequency blue shifts, as observed in the one-dimensional pump–probe data (Figure 8a), but the 2DEV spectra reveal that the line width along the electronic excitation axis also blue shifts and narrows. We have illustrated this for three different waiting times in Figure 11a by plotting the normalized electronic line shape at $\omega_{\text{IR}} = 1583$ cm⁻¹. Cuts for $\omega_{\text{IR}} = 1600$ and 1595 cm⁻¹ returned almost identical traces. To track the time evolution of the electronic axis, we fit the slices at $\omega_{\text{IR}} = 1583$ cm⁻¹ to a Gaussian line shape. The full-width half-maximum (fwhm) and central frequencies returned from the

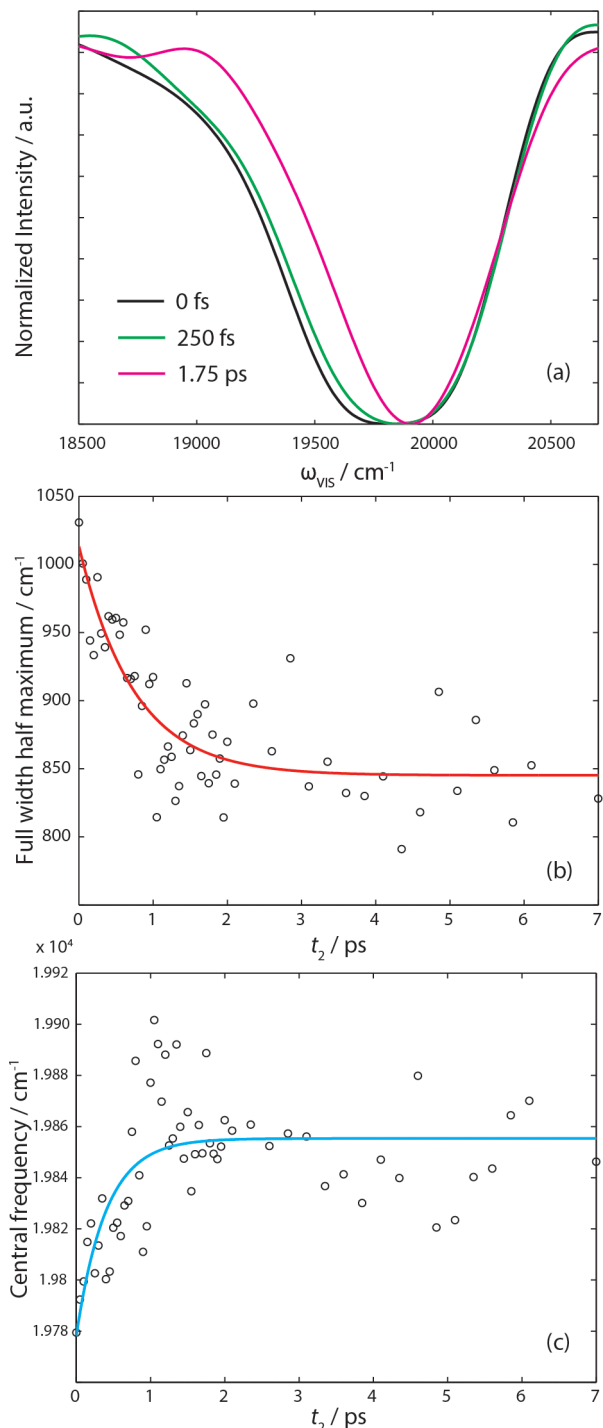


Figure 11. (a) Normalized cut along visible axis for $\omega_{\text{IR}} = 1585 \text{ cm}^{-1}$ for three t_2 delays. Decay of the (b) fwhm and (c) central frequency from fits to the visible line shape.

analysis are plotted in Figure 11b,c, respectively. The decays of these traces were fitted to an exponential decay plus an offset (solid overlaid lines) and reveal the fwhm of the feature along the electronic axis narrows by $\sim 150 \text{ cm}^{-1}$ on a 740 fs time scale, and the central frequency blue shifts by $\sim 80 \text{ cm}^{-1}$ with an associated 400 fs time constant.

Fits to the center line slope along the vertical axis returned a positive correlation between electronic and vibrational degrees of freedom (see overlaid dashed lines on the spectra). Analysis of the CLS revealed a commensurate decay for k_e (cf.

narrowing along the electronic axis) and an associated 750 fs time constant. The positive correlation between electronic and vibrational transition frequencies distributions can be rationalized in terms of correlated baths between the two degrees of freedom; the S_2-S_0 electronic and $v_{\text{C=C}}$ antisymmetric TDMs, displayed in Figure 1a, are parallel, re-enforcing our assignment of this excited state vibration.

The time scale for loss of correlation between electronic and vibrational degrees of freedom is longer than the S_2 lifetime (200 fs), which is worth noting. The long-lived correlation implies that the S_2-S_1 relaxation is ballistic, and the bath must be frozen in the wake of the change in electronic state and associated nuclear configuration. This strongly indicates the action of a conical intersection in, or very close to, the vertical Franck-Condon region.

The dynamical changes of this feature can be explained by considering the following. We recognize that our laser bandwidth (2000 cm^{-1} wing to wing) has sufficient bandwidth to excite one quantum of the probed vibration in the $S_2 \leftarrow S_0$ excitation step, depending on Franck-Condon activity. Alternatively, it may be excited as a consequence of the S_2-S_1 surface crossing. The 2DEV spectra are able to monitor the probe fundamental vibrational transition (and the $2 \leftarrow 1$ overtone) as it evolves on the excited states. The narrowing along the electronic axis likely arises from vibrational cooling of the probed mode on the S_1 electronic state. The simultaneous blue shift on the electronic and IR axis can be explained by the associated change in force constant for this vibration: the bond is stronger on the S_1 state compared to S_0 and S_2 , and therefore the fundamental frequency increases, as per previous *ab initio* calculations for smaller polyenes.⁵²

The long-lived correlation as evidenced in the slow decay of the CLS beyond the S_2 lifetime, and enhanced vibrational activity associated with this vibrational mode, provide evidence to suggest that the antisymmetric $\text{C}=\text{C}$ mode is (one of) the tuning modes at the conical intersection between the S_2 and S_1 states.

Figure 12 displays the 2DEV spectra for the broad double peaked transient centered around 1700 cm^{-1} at four different t_2 waiting times. The peak at $\omega_{\text{IR}} \sim 1720 \text{ cm}^{-1}$ displays a negative center line slope (anticorrelation) along k_e and by analogy with the measurements for cyclohexane, we assign this to the excited state $\text{C}=\text{C}$ symmetric stretching mode.

The feature at 1660 cm^{-1} displays no correlation between electronic and vibration degrees of freedom and is the last of the excited state IR active modes of bapo in the fingerprint region in acetonitrile- d_3 solution to be assigned. The $\text{C}=\text{O}$ ground state stretch is centered at almost the same frequency, 1665 cm^{-1} (Figure 1c). The strong solute-solvent coupling around the polar $\text{C}=\text{O}$ group may lead to a very rapid solvent re-organization, thereby eliminating any electronic-vibrational correlation within our time resolution. Considering these hypotheses thereby allows us to assign this frequency to the excited state $\text{C}=\text{O}$ stretch mode, counter to the congested transient 2DIR exchange measurements by the Righini group.³⁵

d. General Discussion. There are several differences observed for the ultrafast dynamics of bapo in nonpolar cyclohexane compared to polar acetonitrile solutions, which emerge from either static or dynamic effects. To guide this discussion, we have illustrated our proposed reaction mechanisms in Figure 13. Starting with cyclohexane (Figure 13a), we consider the standard model with the three canonical S_0 , S_2 and S_1 states and a high energy ICT state.^{5,12} The double

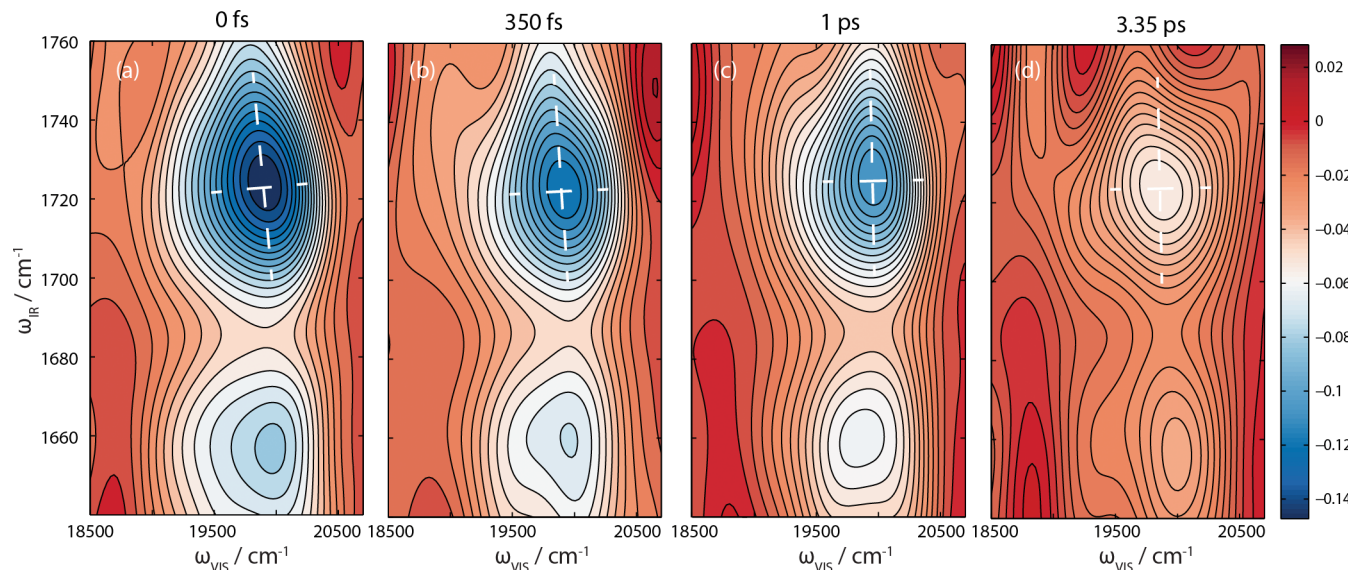


Figure 12. 2DEV spectra for bapo in acetonitrile-*d*₃. The feature centered at 1725 cm⁻¹ is assigned to the C=C symmetric stretch, and that at 1660 cm⁻¹ to the C=O stretch vibrations.

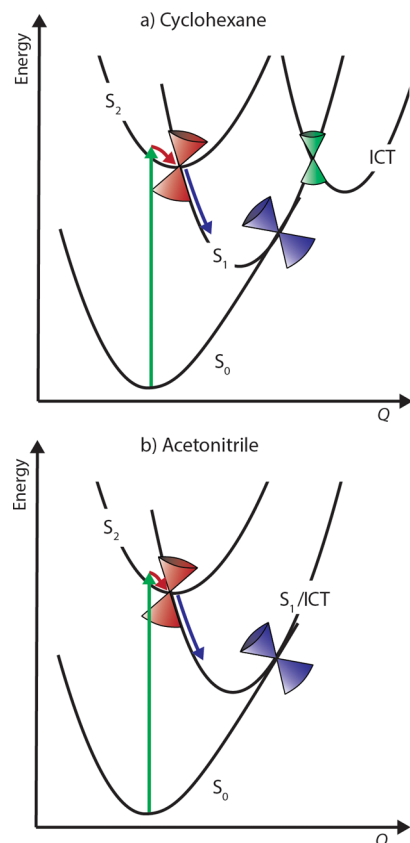


Figure 13. Proposed schematic potential surfaces as a function of reaction coordinate, Q , for the ultrafast dynamics of β -apo-8'-carotenal in (a) cyclohexane and (b) acetonitrile solutions.

cones in the schematic illustrate conical intersections that link the various electronic states; our CLS for the C=C symmetric stretch indicate in cyclohexane there is a conical intersection close to the vertical Franck-Condon region that mediates the ultrafast (300 fs) transfer from S₂ to S₁. From our time-resolved ultrafast visible and infrared probe spectra, we see no evidence for an intermediate dark state between S₂ and S₁ states.

Our results in acetonitrile vary compared to cyclohexane and the schematic is displayed in Figure 13b. We have depicted the S₁ and ICT state as one electronic manifold in this picture, as our mid-IR probe studies reveal that the S₁ and ICT states (thought to both have A_g⁻ symmetry) are either completely mixed or constitute a single electronic state, as evidenced by the immediately broad vibrational line shapes associated with the C=C symmetric and C=O excited state stretches. For acetonitrile, we have drawn the CI between the S₂ and S₁ states as being closer to the vertical Franck-Condon region than in cyclohexane based on the shorter (by 100 fs) S₂ lifetime. The slow loss of correlation between electronic and vibrational transition frequencies for the C=C antisymmetric stretching mode, and enhanced vibrational activity associated with this excited state vibration, point toward this being (one of) the tuning modes at the CI between the S₂ and S₁ states, and therefore the reaction coordinate, Q , in our schematic.

The role of conical intersections driving a ballistic S₂ → S₁ transfer is not a new concept,^{19–21} and studies of β -carotene using broadband impulsive vibrational spectroscopy (BBVIS) by Liebel et al. demonstrated wavepackets associated with backbone modes are conserved upon S₂ → S₁ transfer,²¹ suggesting that activity associated with these nuclear motions might mean that the associated nuclear motions are the tuning modes at the CI. We note that conservation of nuclear wavepackets between two different electronic states does not necessarily indicate the nuclear motions associated with the observed vibrational wavepackets are the tuning modes, and may in fact be created in the S₂ state and act as spectators to the surface crossing, lying in an orthogonal dimension. The notable advantages that 2DEV has over the other spectroscopies such as BBVIS, is the vibrational frequencies can be determined on the excited state as the reaction proceeds, instead of averaging over the entire t_2 decay. Further, physical insights, as we have demonstrated, can be gained from the sign and time scale for decay of the CLS.

4. CONCLUSIONS

We have studied the ultrafast relaxation dynamics of β -apo-8'-carotenal in acetonitrile and cyclohexane solutions with

transient absorption, one- and two-dimensional electronic-vibrational spectroscopy. Our one-dimensional TA and mid-IR probe results are in good agreement with previous studies;^{30,32–34} however, with shorter pump pulse durations we are able to capture the earliest time epoch of the model carotenol system, monitoring the decay of molecules from the S₂ electronic state. We observe static and dynamical differences between bapo in cyclohexane and acetonitrile solutions, most notable are the line shapes associated with the C=O symmetric stretch, are influenced greatly by the coupling of the S₁ and intramolecular charge-transfer state in acetonitrile. From our 2DEV measurements and fits to the center line slopes, we are able to offer more definitive assignments of excited state vibrations in acetonitrile solution. Our polarization anisotropy measurements in both solutions demonstrate that bapo does not undergo any immediate excited state *trans*-*cis* isomerization in either solvent studied, counter to prior hypotheses.^{32,33,39,40} The 2DEV measurements provide *direct* evidence for ballistic transfer of molecules between the S₂ and S₁ states, mediated via a conical intersection very close to the vertical Franck–Condon region. In acetonitrile, given vibrational excitation and the slow decay of the CLS compared to the S₂ lifetime, we propose that the C=C antisymmetric stretch is one of the tuning modes at the conical intersection connecting the S₂ and S₁ states.

To further our understanding of the complex nonradiative relaxation dynamics of carotenoids and carotenals of chain lengths relevant to biological systems, we need a fuller (and accurate) description of the excited potential energy surfaces, specifically the character of the electronic states, their energetic ordering and the geometries that interconnect them. The best efforts to date^{53,66} have only managed to capture the vertical excitation energies, but as this and many other studies have shown, it is a very multidimensional problem. We hope that our 2DEV measurements will spur on advances in theoretical calculations and provide a new benchmark for the detail that experiments can probe in complex nonradiative dynamics. One obvious extension to the 2DEV spectroscopy presented here would be excite the S₁ state directly via two-photon absorption, prior to mid-IR probe, thus allowing for direct electronic-vibrational correlations in the S₁ state. BBVIS as championed by the group of Kukura^{21,67} has already provided insights into the anharmonic coupling and coherent nuclear motion mediating S₂/S₁ coupling in β-carotene. Applying BBIVS to β-apo-8'-carotenol in solvents of different polarities could potentially provide complementary information to the 2DEV data presented here, and thus further improve our understanding of the complex nonradiative decay pathways of bapo.

ASSOCIATED CONTENT

Supporting Information

Full broadband visible pump, mid-IR probe data sets are given in the Supporting Information. The Supporting Information is available free of charge on the ACS Publications website at DOI: 10.1021/acs.jpcb.5b04893.

AUTHOR INFORMATION

Corresponding Author

*G. R. Fleming. E-mail: grfleming@lbl.gov. Tel: (510) 643-2735. Fax: (510) 642-6340.

Notes

The authors declare no competing financial interest.

ACKNOWLEDGMENTS

The authors thank Hui Dong and Nicholas Lewis for useful discussions. This work was supported by the National Science Foundation (NSF) under Contract CHE-1012168. We are also grateful to the College of Chemistry Molecular Graphics facility, which is funded by NSF under Contract CHE-0840505.

REFERENCES

- (1) Bode, S.; Quentmeier, C. C.; Liao, P.-N.; Hafi, N.; Barros, T.; Wilk, L.; Bittner, F.; Walla, P. J. On the Regulation of Photosynthesis by Excitonic Interactions Between Carotenoids and Chlorophylls. *Proc. Natl. Acad. Sci. U. S. A.* **2009**, *106*, 12311–12316.
- (2) Siefermann-Harms, D. The Light-Harvesting and Protective Functions of Carotenoids in Photosynthetic Membranes. *Physiol. Plant.* **1987**, *69*, 561–568.
- (3) Walla, P. J.; Linden, P. A.; Hsu, C. P.; Scholes, G. D.; Fleming, G. R. Femtosecond Dynamics of the Forbidden Carotenoid S₁ State in Light-Harvesting Complexes of Purple Bacteria Observed after Two-Photon Excitation. *Proc. Natl. Acad. Sci. U. S. A.* **2000**, *97*, 10808–10813.
- (4) Demmig-Adams, B. Carotenoids and Photoprotection in Plants: a Role for the Xanthophyll Zeaxanthin. *Biochim. Biophys. Acta, Bioenerg.* **1990**, *1020*, 1–24.
- (5) Polívka, T.; Sundström, V. Ultrafast Dynamics of Carotenoid Excited States—From Solution to Natural and Artificial Systems. *Chem. Rev.* **2004**, *104*, 2021–2072.
- (6) Polívka, T.; Sundström, V. Dark Excited States of Carotenoids: Consensus and Controversy. *Chem. Phys. Lett.* **2009**, *477*, 1–11.
- (7) Jailaubekov, A. E.; Vengris, M.; Song, S.-H.; Kusumoto, T.; Hashimoto, H.; Larsen, D. S. Deconstructing the Excited-State Dynamics of β-Carotene in Solution. *J. Phys. Chem. A* **2011**, *115*, 3905–3916.
- (8) Ostroumov, E. E.; Mulvaney, R. M.; Cogdell, R. J.; Scholes, G. D. Broadband 2D Electronic Spectroscopy Reveals a Carotenoid Dark State in Purple Bacteria. *Science* **2013**, *340*, 52–56.
- (9) Lukeš, V.; Christensson, N.; Milota, F.; Kauffmann, H. F.; Hauer, J. Electronic Ground State Conformers of β-Carotene and Their Role in Ultrafast Spectroscopy. *Chem. Phys. Lett.* **2011**, *506*, 122–127.
- (10) Cerón-Carrasco, J. P.; Requena, A.; Marian, C. M. Theoretical Study of the Low-Lying Excited States of β-Carotene Isomers by a Multireference Configuration Interaction Method. *Chem. Phys.* **2010**, *373*, 98–103.
- (11) Zigmantas, D.; Hiller, R. G.; Sharples, F. P.; Frank, H. A.; Sundström, V.; Polívka, T. Effect of a Conjugated Carbonyl Group on the Photophysical Properties of Carotenoids. *Phys. Chem. Chem. Phys.* **2004**, *6*, 3009–3016.
- (12) Frank, H. A.; Bautista, J. A.; Josue, J.; Pendon, Z.; Hiller, R. G.; Sharples, F. P.; Gosztola, D.; Wasielewski, M. R. Effect of the Solvent Environment on the Spectroscopic Properties and Dynamics of the Lowest Excited States of Carotenoids. *J. Phys. Chem. B* **2000**, *104*, 4569–4577.
- (13) De Re, E.; Schlau-Cohen, G. S.; Leverenz, R. L.; Huxter, V. M.; Oliver, T. A. A.; Mathies, R. A.; Fleming, G. R. Insights Into the Structural Changes Occurring Upon Photoconversion in the Orange Carotenoid Protein From Broadband Two-Dimensional Electronic Spectroscopy. *J. Phys. Chem. B* **2014**, *118*, 5382–5389.
- (14) Kopczynski, M.; Ehlers, F.; Lenzer, T.; Oum, K. Evidence for an Intramolecular Charge Transfer State in 12'-Apo-β-Caroten-12'-Al and 8'-Apo-β-Caroten-8'-Al: Influence of Solvent Polarity and Temperature. *J. Phys. Chem. A* **2007**, *111*, 5370–5381.
- (15) Ehlers, F.; Wild, D. A.; Lenzer, T.; Oum, K. Investigation of the S₁/ICT → S₀ Internal Conversion Lifetime of 4'-Apo-β-Caroten-4'-Al and 8'-Apo-β-Caroten-8'-Al: Dependence on Conjugation Length and Solvent Polarity. *J. Phys. Chem. A* **2007**, *111*, 2257–2265.
- (16) Durcan, M.; Fuciman, M.; Slouf, V.; Keşan, G.; Polívka, T. Excited-State Dynamics of Monomeric and Aggregated Carotenoid 8'-Apo-β-Carotenol. *J. Phys. Chem. A* **2012**, *116*, 12330–12338.

- (17) Macernis, M.; Sulskus, J.; Duffy, C. D. P.; Ruban, A. V.; Valkunas, L. Electronic Spectra of Structurally Deformed Lutein. *J. Phys. Chem. A* **2012**, *116*, 9843–9853.
- (18) Bautista, J. A.; Connors, R. E.; Raju, B. B.; Hiller, R. G.; Sharples, F. P.; Gosztola, D.; Wasielewski, M. R.; Frank, H. A. Excited State Properties of Peridinin: Observation of a Solvent Dependence of the Lowest Excited Singlet State Lifetime and Spectral Behavior Unique Among Carotenoids. *J. Phys. Chem. B* **1999**, *103*, 8751–8758.
- (19) Fuss, W.; Haas, Y.; Zilberg, S. Twin States and Conical Intersections in Linear Polyenes. *Chem. Phys.* **2000**, *259*, 273–295.
- (20) Kukura, P.; McCamant, D. W.; Mathies, R. A. Femtosecond Time-Resolved Stimulated Raman Spectroscopy of the S_2 $1B_u$ Excited State of β -Carotene. *J. Phys. Chem. A* **2004**, *108*, 5921–5925.
- (21) Liebel, M.; Schnedermann, C.; Kukura, P. vibrationally Coherent Crossing and Coupling of Electronic States During Internal Conversion in β -Carotene. *Phys. Rev. Lett.* **2014**, *112*, 198302.
- (22) Herzberg, G.; Longuet-Higgins, H. C. Intersection of Potential Energy Surfaces in Polyatomic Molecules. *Discuss. Faraday Soc.* **1963**, *35*, 77–82.
- (23) *Conical Intersections: Electronic Structure, Dynamics and Spectroscopy*; Domcke, W., Yarkony, D. R., Köppel, H., Eds.; World Scientific: Singapore, 2004.
- (24) Nakayama, K.; Nakano, H.; Hirao, K. Theoretical Study of the $\pi \rightarrow \pi^*$ Excited States of Linear Polyenes: the Energy Gap Between $1^1B_u^+$ And $2^1A_g^-$ States and Their Character. *Int. J. Quantum Chem.* **1998**, *66*, 157–175.
- (25) Garavelli, M.; Celani, P.; Bernardi, F.; Robb, M. A.; Olivucci, M. Force Fields for “Ultrafast” Photochemistry: the S_2 ($1B_u$) $\rightarrow S_1$ ($2A_g$) $\rightarrow S_0$ ($1A_g$) Reaction Path for All-Trans-Hexa-1, 3, 5-Triene. *J. Am. Chem. Soc.* **1997**, *119*, 11487–11494.
- (26) Garavelli, M.; Bernardi, F.; Olivucci, M.; Vreven, T.; Klein, S. P.; Celani, P.; Robb, M. A. Potential-Energy Surfaces for Ultrafast Photochemistry Static and Dynamic Aspects. *Faraday Discuss.* **1998**, *110*, 51–70.
- (27) Christensson, N.; Milota, F.; Nemeth, A.; Sperling, J.; Kauffmann, H. F.; Pullerits, T.; Hauer, J. Two-Dimensional Electronic Spectroscopy of β -Carotene. *J. Phys. Chem. B* **2009**, *113*, 16409–16419.
- (28) Calhoun, T. R.; Davis, J. A.; Graham, M. W.; Fleming, G. R. The Separation of Overlapping Transitions in β -Carotene with Broadband 2D Electronic Spectroscopy. *Chem. Phys. Lett.* **2012**, *523*, 1–5.
- (29) Pang, Y.; Jones, G. A.; Prantil, M. A.; Fleming, G. R. Unusual Relaxation Pathway From the Two-Photon Excited First Singlet State of Carotenoids. *J. Am. Chem. Soc.* **2010**, *132*, 2264–2273.
- (30) Pang, Y.; Fleming, G. R. Branching Relaxation Pathways From the Hot S_2 State of 8'-Apo- β -Caroten-8'-Al. *Phys. Chem. Chem. Phys.* **2010**, *12*, 6782–6788.
- (31) Pang, Y.; Prantil, M. A.; Van Tassel, A. J.; Jones, G. A.; Fleming, G. R. Excited-State Dynamics of 8'-Apo- β -Caroten-8'-Al and 7',7'-Dicyano-7'-Apo- β -Carotene Studied by Femtosecond Time-Resolved Infrared Spectroscopy. *J. Phys. Chem. B* **2009**, *113*, 13086–13095.
- (32) Di Donato, M.; Segado Centellas, M.; Lapini, A.; Lima, M.; Avila, F.; Santoro, F.; Cappelli, C.; Righini, R. Combination of Transient 2D-IR Experiments and *Ab Initio* Computations Sheds Light on the Formation of the Charge-Transfer State in Photoexcited Carbonyl Carotenoids. *J. Phys. Chem. B* **2014**, *118*, 9613–9630.
- (33) Ragnoni, E.; Di Donato, M.; Iagatti, A.; Lapini, A.; Righini, R. Mechanism of the Intramolecular Charge Transfer State Formation in All-Trans- β -Apo-8'-Carotenal: Influence of Solvent Polarity and Polarizability. *J. Phys. Chem. B* **2015**, *119*, 420–432.
- (34) Di Donato, M.; Ragnoni, E.; Lapini, A.; Kardaś, T. M.; Ratajska-Gadomska, B.; Foggi, P.; Righini, R. Identification of the Excited State C=C and C=O Modes of Trans- β -Apo-8'-Carotenal with Transient 2D-IR-EXSY and Femtosecond Stimulated Raman Spectroscopy. *J. Phys. Chem. Lett.* **2015**, *6*, 1592–1598.
- (35) Kardaś, T. M.; Ratajska-Gadomska, B.; Lapini, A.; Ragnoni, E.; Righini, R.; Di Donato, M.; Foggi, P.; Gadomski, W. Dynamics of the Time-Resolved Stimulated Raman Scattering Spectrum in Presence of Transient Vibronic Inversion of Population on the Example of
- Optically Excited Trans- β -Apo-8'-Carotenal. *J. Chem. Phys.* **2014**, *140*, 204312.
- (36) Oliver, T. A. A.; Lewis, N. H. C.; Fleming, G. R. Correlating the Motion of Electrons and Nuclei with Two-Dimensional Electronic-Vibrational Spectroscopy. *Proc. Natl. Acad. Sci. U. S. A.* **2014**, *111*, 10061–10066 (also see corrections on page 16628).
- (37) Tscherner, N.; Schenderlein, M.; Brose, K.; Schlodder, E.; Mroginski, M. A.; Thomsen, C.; Hildebrandt, P. Resonance Raman Spectra of β -Carotene in Solution and in Photosystems Revisited: an Experimental and Theoretical Study. *Phys. Chem. Chem. Phys.* **2009**, *11*, 11471–11478.
- (38) Banerjee, S.; Kröner, D.; Saalfrank, P. Resonance Raman and Vibronic Absorption Spectra with Duschinsky Rotation From a Time-Dependent Perspective: Application to β -Carotene. *J. Chem. Phys.* **2012**, *137*, 22A534.
- (39) Niedzwiedzki, D.; Koscielecki, J. F.; Cong, H.; Sullivan, J. O.; Gibson, G. N.; Birge, R. R.; Frank, H. A. Ultrafast Dynamics and Excited State Spectra of Open-Chain Carotenoids at Room and Low Temperatures. *J. Phys. Chem. B* **2007**, *111*, 5984–5998.
- (40) Cong, H.; Niedzwiedzki, D. M.; Gibson, G. N.; LaFountain, A. M.; Kelsh, R. M.; Gardiner, A. T.; Cogdell, R. J.; Frank, H. A. Ultrafast Time-Resolved Carotenoid to-Bacteriochlorophyll Energy Transfer in LH2 Complexes From Photosynthetic Bacteria. *J. Phys. Chem. B* **2008**, *112*, 10689–10703.
- (41) Dong, H.; Lewis, N. H. C.; Oliver, T. A. A.; Fleming, G. R. Determining the Static Electronic and Vibrational Energy Correlations via Two-Dimensional Electronic-Vibrational Spectroscopy. *J. Chem. Phys.* **2015**, *142*, 174201.
- (42) Lewis, N. H.; Dong, H.; Oliver, T. A. A.; Fleming, G. R. Measuring Correlated Electronic and Vibrational Spectral Dynamics Using Line Shapes in Two-Dimensional Electronic-Vibrational Spectroscopy. *J. Chem. Phys.* **2015**, *142*, 174202.
- (43) Tournois, P. Acousto-Optic Programmable Dispersive Filter for Adaptive Compensation of Group Delay Time Dispersion in Laser Systems. *Opt. Commun.* **1997**, *140*, 245–249.
- (44) Oksenhendler, T.; Coudreau, S.; Forget, N.; Crozatier, V.; Grabielle, S.; Herzog, R.; Gobert, O.; Kaplan, D. Self-Referenced Spectral Interferometry. *Appl. Phys. B: Lasers Opt.* **2010**, *99*, 7–12.
- (45) Demirdöven, N.; Khalil, M.; Golonzka, O.; Tokmakoff, A. Dispersion Compensation with Optical Materials for Compression of Intense Sub-100-fs Mid-Infrared Pulses. *Opt. Lett.* **2002**, *27*, 433–435.
- (46) Shao, Y.; Molnar, L. F.; Jung, Y.; Kussmann, J. R.; Ochsenfeld, C.; Brown, S. T.; Gilbert, A. T. B.; Slipchenko, L. V.; Levchenko, S. V.; O'Neill, D. P.; et al. Advances in Methods and Algorithms in a Modern Quantum Chemistry Program Package. *Phys. Chem. Chem. Phys.* **2006**, *8*, 3172–3191.
- (47) Krylov, A. I.; Gill, P. M. W. Q-Chem: an Engine for Innovation. *Comput. Mol. Sci.* **2013**, *3*, 317–326.
- (48) Cerón-Carrasco, J. P.; Bastida, A.; Zúñiga, J.; Requena, A.; Miguel, B. Density Functional Theory Study of the Stability and Vibrational Spectra of the β -Carotene Isomers. *J. Phys. Chem. A* **2009**, *113*, 9899–9907.
- (49) Cerezo, J.; Zúñiga, J.; Bastida, A.; Requena, A.; Cerón-Carrasco, J. P.; Eriksson, L. A. Antioxidant Properties of B-Carotene Isomers and Their Role in Photosystems: Insights From Ab Initio Simulations. *J. Phys. Chem. A* **2012**, *116*, 3498–3506.
- (50) von Doering, W.; Sotiriou-Leventis, C.; Roth, W. R. Thermal Interconversions Among 15-Cis-, 13-Cis-, and All-Trans- β -Carotene: Kinetics, Arrhenius Parameters, Thermochemistry, and Potential Relevance to Anticarcinogenicity of All-Trans- β -Carotene. *J. Am. Chem. Soc.* **1995**, *117*, 2747–2757.
- (51) Snellenburg, J. J.; Laptenok, S. P.; Seger, R.; Mullen, K. M.; van Stokkum, I. H. M. Glotaran: a Java-Based Graphical User Interface for the R Package TIMP. *J. Stat. Software* **2012**, *49*, 1–22.
- (52) Zerbetto, F.; Zgierski, M. Z.; Negri, F.; Orlandi, G. Theoretical Study of the Force Fields of the Three Lowest Singlet Electronic States of Linear Polyenes. *J. Chem. Phys.* **1988**, *89*, 3681–3688.

- (53) Kleinschmidt, M.; Marian, C. M.; Waletzke, M.; Grimme, S. Parallel Multireference Configuration Interaction Calculations on Mini- β -Carotenes and β -Carotene. *J. Chem. Phys.* **2009**, *130*, 044708.
- (54) Ghosh, D.; Hachmann, J.; Yanai, T.; Chan, G. K.-L. Orbital Optimization in the Density Matrix Renormalization Group, with Applications to Polyenes and β -Carotene. *J. Chem. Phys.* **2008**, *128*, 144117.
- (55) Hamm, P. Coherent Effects in Femtosecond Infrared Spectroscopy. *Chem. Phys.* **1995**, *200*, 415–429.
- (56) Wynne, K.; Hochstrasser, R. M. The Theory of Ultrafast Vibrational Spectroscopy. *Chem. Phys.* **1995**, *193*, 211–236.
- (57) Birge, R. R.; Zgierski, M. Z.; Serrano-Andres, L.; Hudson, B. S. Transition Dipole Orientation of Linear Polyenes: Semiempirical Models and Extrapolation to the Infinite Chain Limit. *J. Phys. Chem. A* **1999**, *103*, 2251–2255.
- (58) Tao, T. Time-Dependent Fluorescence Depolarization and Brownian Rotational Diffusion Coefficients of Macromolecules. *Biopolymers* **1969**, *8*, 609–632.
- (59) Kwak, K.; Park, S.; Finkelstein, I. J.; Fayer, M. D. Frequency-Frequency Correlation Functions and Apodization in Two-Dimensional Infrared Vibrational Echo Spectroscopy: a New Approach. *J. Chem. Phys.* **2007**, *127*, 124503.
- (60) Kwak, K.; Rosenfeld, D. E.; Fayer, M. D. Taking Apart the Two-Dimensional Infrared Vibrational Echo Spectra: More Information and Elimination of Distortions. *J. Chem. Phys.* **2008**, *128*, 204505.
- (61) Kwac, K.; Cho, M. Two-Color Pump-Probe Spectroscopies of Two-and Three-Level Systems: 2-Dimensional Line Shapes and Solvation Dynamics. *J. Phys. Chem. A* **2003**, *107*, 5903.
- (62) Takaya, T.; Iwata, K. Relaxation Mechanism of β -Carotene From $S_2(1B_u^+)$ State to $S_1(2A_g^-)$ State: Femtosecond Time-Resolved Near-IR Absorption and Stimulated Resonance Raman Studies in 900–1550 nm Region. *J. Phys. Chem. A* **2014**, *118*, 4071–4078.
- (63) Khalil, M.; Demirdöven, N.; Tokmakoff, A. Coherent 2D IR Spectroscopy: Molecular Structure and Dynamics in Solution. *J. Phys. Chem. A* **2003**, *107*, 5258–5279.
- (64) Pisliakov, A. V.; Mančal, T.; Fleming, G. R. Two-Dimensional Optical Three-Pulse Photon Echo Spectroscopy. II. Signatures of Coherent Electronic Motion and Exciton Population Transfer in Dimer Two-Dimensional Spectra. *J. Chem. Phys.* **2006**, *124*, 234505.
- (65) Terenziani, F.; Painelli, A. Two-Dimensional Electronic-Vibrational Spectra: Modeling Correlated Electronic and Nuclear Motion. *Phys. Chem. Chem. Phys.* **2015**, *17*, 13074–13081.
- (66) Andreussi, O.; Knecht, S.; Marian, C. M.; Kongsted, J.; Mennucci, B. Carotenoids and Light-Harvesting: From DFT/MRCI to the Tamm-Dancoff Approximation. *J. Chem. Theory Comput.* **2015**, *11*, 655–666.
- (67) Liebel, M.; Kukura, P. Broad-Band Impulsive Vibrational Spectroscopy of Excited Electronic States in the Time Domain. *J. Phys. Chem. Lett.* **2013**, *4*, 1358–1364.